6th European Conference on Computational Mechanics (ECCM 6)
7th European Conference on Computational Fluid Dynamics (ECFD 7)
11 – 15 June 2018, Glasgow, UK

NUMERICAL MODELLING AND EXPERIMENTATION OF HISTORICAL CARPENTRY CORNER LOG JOINTS

ANNA PESTKA[1], KATARZYNA SZEPIETOWSKA[2], PAWEŁ KŁOSOWSKI[3], MARCIN KRAJEWSKI[4] AND IZABELA LUBOWIECKA[5]

Gdańsk University of Technology, Faculty of Civil and Environmental Engineering,
Department of Structural Mechanics
11/12 Gabriela Narutowicza Street, 80-233 Gdańsk, Poland
[1]annmlecz@pg.edu.pl, [2]katszepi@pg.edu.pl, [3]klosow@pg.edu.pl, [4]markraje@pg.edu.pl,
[5]lubow@pg.edu.pl,

Key words: carpentry joints, short-corner dovetail connection, saddle notch joint, orthotropic material, finite element models.

Abstract. The main purpose of this research is to determine the stress distributions on the contact surfaces between the logs of the historical carpentry corner joints. The additional purpose is to compare the stress distribution for four different boundary conditions in the case of dry and wet pine wood. The paper presents the results of numerical analysis of the short-corner dovetail connection and the saddle notch corner joint, which are in common use in currently preserved objects of wooden architecture. The wood has been modelled as an orthotropic material. The numerical calculations have been carried out using MSC.Marc/Mentat software. The knowledge about the damage zones in the connections is immensely important, due to the need for maintenance, renovation and the reinforcement of existing elements in many timber historic buildings.

1 INTRODUCTION

Historically, wood was widely used in the construction of structures due to good strength parameters and the wide availability of the material. Timber structures are more complicated in analysis and design than steel o concrete structure due to heterogeneity of the material [1] and its sensitivity to moisture and biological damage [2, 3]. As reported in literature, its strength and flexibility depend on humidity, temperature, density and aging [4, 5]. Currently, more attention is focused on restoring valuable historical buildings [6], and therefore there is a need for reliable structural modelling and analysis that could be the basis for an effective repair to ensure the safety of the structure.

The development of carpentry, dated to the period from the 13th to 17th century, contributed to significant improvements in joining techniques that resulted in a number of new types of carpentry joints. Some modifications developed within those centuries mainly consisted of changing the geometry and the introduction of locks inside the joint, sometimes in a very complex form [7, 8].

Depending on the form and expected functions many types of carpentry joints can be distinguished [9, 10]. A lot of them have been studied and presented in research papers (see e.g., [11, 12]) but the vast majority of them concern the analysis of typical joinery in the historic roof structures. In general the timebr structures are anlaysed in terms of experimentation [13–16], numerical analysis [17–22] and also about temperature and humidity effect on the strength of wood [23–25]. Some studies on the stress state and failure analysis of timber structures can also be found in [11, 26, 27].

Despite their popularity in historical buildings, it is difficult to find research on the carpentry connections of wall corners in log buildings (see e.g., [28]). And it would be extremely important for proper maintenance, renovation and strengthening of existing elements in many historic wooden structures [29].

This study presents some aspects of numerical modelling and analysis of the historic carpentry corner wall connections. Two types of joints are analysed, a short-corner dovetail connection, and a saddle notch joint. Different boundary conditions and different load systems are applied to perform the finite element analysis. The main goal of the analysis is to find the stress distribution in the loaded wall with traditional carpentry joints constructed from logs in different ways, to simulate their mechanical performance. The material parameters of the wood taken into the analysis come from 4-point bending tests.

2 MATERIALS AND METHODS

2.1 Geometry of short-corner dovetail connection and material parameters

The geometry of the connections can be varied depending on the place and time of the object's construction in which the connections are used. In the paper, the dimensions of the analysed connections have been scaled into 1:2 in relation to the geometry described by [30]. The analysed carpentry joints consist of five logs. The cross-section dimensions of a single wooden beam are 75 x 135 mm. The length of each log is 1000 mm for the short-corner dovetail connection. In turn, the length of each log is 1075 mm for the saddle notch corner joint. The geometry of the short-corner dovetail connection and the saddle notch corner joint haves been presented in figure 1.

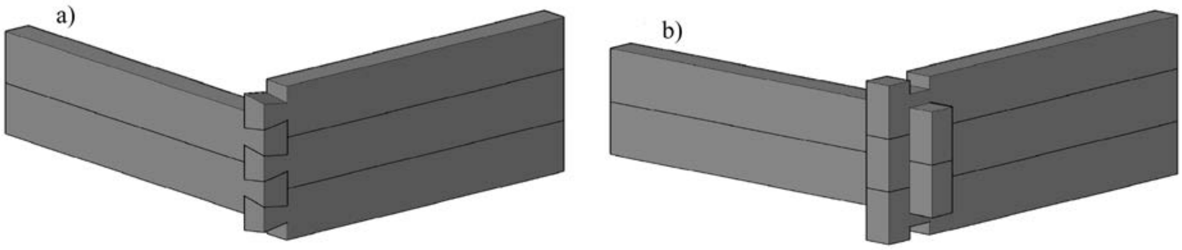

Figure 1: Geometry of carpentry joints: a) short-corner dovetail connection, b) saddle notch corner joint

The material of the joints has been modelled as a pine wood. Due to the dependency of the material properties on the directions of the wood fibres, the pine wood has been defined as an orthotropic material. The numerical calculations have been performed in two variants of moisture (dry and wet wood). The measured wood moisture for the dry wood was approximately 10%, in turn for the wet wood approximately 21%. The value of the longitudinal elastic modulus E_L has been calculated on the basis of the 4-point bending tests. Another parameters have been estimated based on [1] in relation to the values of the longitudinal elastic modulus. The material parameters of pine wood for the wood moisture 10% and 21% are presented in table 1, where *L* represents longitudinal direction, *T*- tangential direction and *R* – radial direction of the wood. The 4-piont bending tests have been carried out on specimens of approximately 300 mm of active length.

Table 1: Material parameters of pine wood

Material constant	Value for dry wood (10%)	Value for wet wood (21%)	Unit
E_L	$1.23\cdot10^{10}$	$7.85\cdot10^{9}$	Pa
E_R	$1.25\cdot10^{9}$	$8.01\cdot10^{8}$	Pa
E_T	$8.35\cdot10^{8}$	$5.34\cdot10^{8}$	Pa
G_{RT}	$6.14\cdot10^{7}$	$3.93\cdot10^{7}$	Pa
G_{TL}	$5.65\cdot10^{8}$	$3.61\cdot10^{8}$	Pa
G_{LR}	$6.02\cdot10^{8}$	$3.85\cdot10^{8}$	Pa
ν_{RT}	0.469	0.469	-
ν_{TL}	0.024	0.024	-
ν_{LR}	0.316	0.316	-

The cross-section dimensions of the specimens have been approximately 40 mm by 20 mm. The scheme of the test has been presented in figure 2.

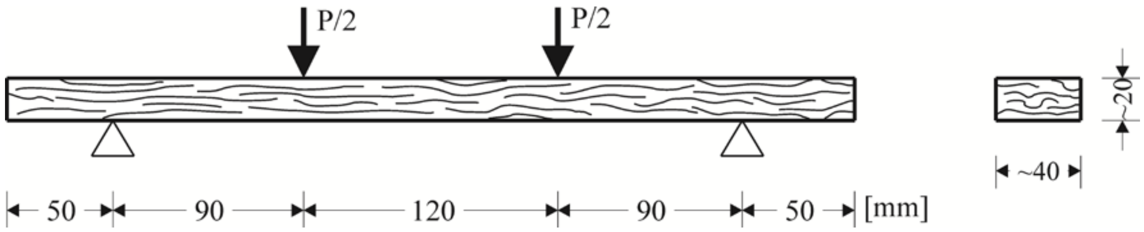

Figure 2: Scheme of the laboratory stand of 4-point bending tests

2.2 Numerical analysis

The numerical nonlinear static analysis has been performed using MSC.Marc/Mentat software. The finite element method has been applied in modelling of the analysed connections. The numerical model of the short-corner dovetail joint has been built using approximately 61000 solid tetra elements while the saddle notch corner joint has been modelled using approximately 101000 solid tetra elements. The finite element mesh has been adequately refined in the connections' corners. The contact between the individual elements of the joints has been taken into account in the analysis. The friction coefficient between logs has been assumed as 0.25 for the dry wood and 0.2 for the wet wood.

The numerical simulations have been carried out for four different boundary conditions in order to select the most resistant type of the connection and to determine the stress distributions in the connections' corners. The types of boundary conditions applied in the analysed carpentry joint have been presented in table 2. For all types of the boundary conditions, the external surfaces of most bottom logs have been fixed in the direction Z. In turn, the external surfaces for most top logs have been loaded with the pressure of 13019.2 N/m^2 for the dry wood and 14707.6 N/m^2 for the wet wood. The values of pressure have been calculated as the dead load of approximately 2.5 m high typical wall. The height of 2.5 m corresponds to the nineteen logs lying above.

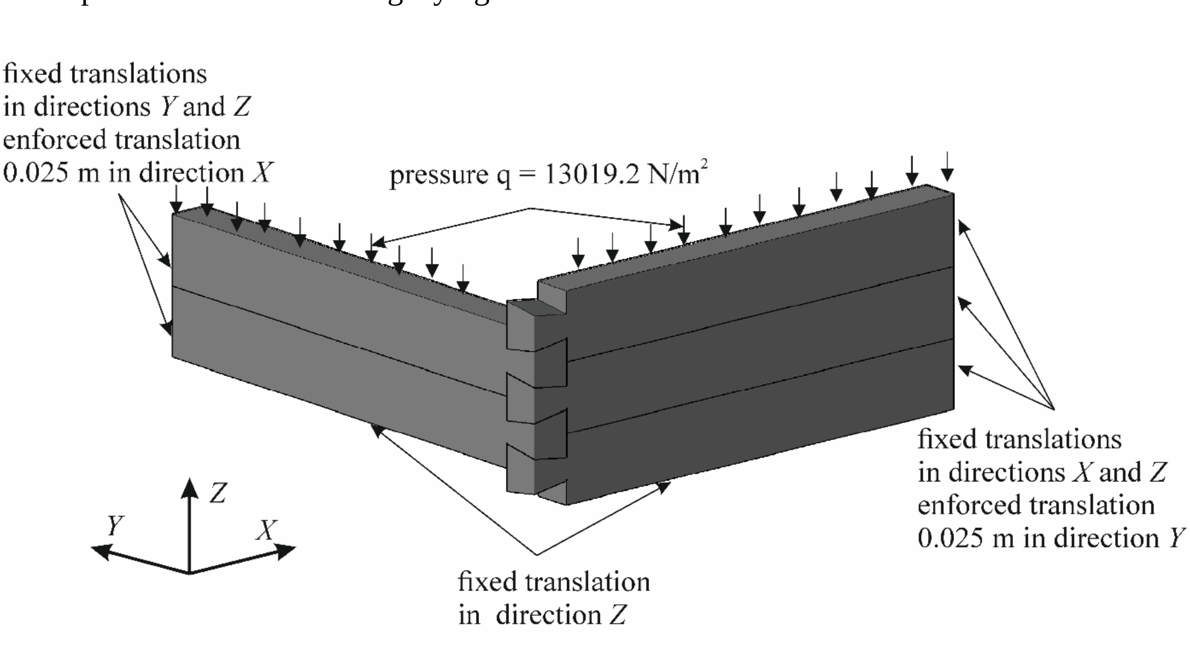

Figure 3: Boundary conditions applied in Type 1 for dry pine wood

The remaining boundary conditions depend on the type of performed analysis and are described in table 2. The exemplary boundary conditions applied in Type 1 for the dry wood of the short-corner dovetail connection have been presented in figure 3. The deformations of the wooden beams in the carpentry connections are very dangerous for the structure when they are large (e.g. because of possibility of biological damage). Different boundary conditions (including assumed structure displacements) can lead to such large deformations. So it has been decided to test different boundary conditions, shown in table 2, in the simulations of the joints behaviour.

Table 2: Types of boundary conditions applied in analysed carpentry joint

	At the end of two logs		At the end of three logs	
	Fixed displacement (direction)	Enforced displacement (value and direction)	Fixed displacement (direction)	Enforced displacement (value and direction)
Type 1	*Y* and *Z*	0.025 m, *X*	*X* and *Z*	0.025 m, *Y*
Type 2	*Y* and *Z*	–0.025 m, *X*	*X* and *Z*	–0.025 m, *Y*
Type 3	*X* and *Z*	0.025 m, *Y*	*Y* and *Z*	0.025 m, *X*
Type 4	*X* and *Z*	–0.025 m, *Y*	*Y* and *Z*	–0.025 m, *X*

3 RESULTS AND DISCUSSION

The results of the static analysis of short-corner dovetail connection and the saddle notch corner joint obtained taking into account the four different types of boundary conditions are compared in this study. The first important finding of the analysed joints is that there are the same major principal values of stress and high stress areas for Types 1 and 4, and for Types 2 and 3 of the boundary conditions for both dry and wet pine wood and for both carpentry joints types. It has been noted that both minimum and maximum principal values of stress are the highest for the wet pine wood for the short-corner dovetail connection (figures 4-7). In turn, for the saddle notch joint, both minimum and maximum principal values of stress are the highest for the dry pine wood.

The minimal principal stress in the short-corner dovetail connection made of wet wood is distributed symmetrically (Types 1 and 4) and the highest stress areas are concentrated along the edges of the logs (figure 4). The same situation is in the case of the saddle notch corner joint (figure 8). The minimum principal values of stress are much lower in case of dry pine wood with the same type of boundary conditions than in case of the wet wood for the short corner dovetail connection (figure 4-5). The high stress areas are also smaller, but concentrated along the edges of the logs like in case of the dry wood (figure 4a). The minimum principal values of stress for Type 2 of boundary conditions are smaller (< 43 MPa) than for Type 1 in both cases, dry and wet pine wood. In the case of the saddle notch corner joint, the situation gives the opposite result. The minimum principal values of stress is much lower in the case of wet pine wood with the same type of boundary conditions than in the case of the dry wood (figure 8-9). The areas of the highest stress are larger in the case of dry wood in relation to the wet wood. In turn, the minimum principal values of stress for Type 2 of boundary conditions are lower than for Type 1 in both cases, the dry and the wet pine wood, as for the short-corner dovetail connection.

It has been observed that in the short-corner dovetail connection, the maximum principal stress distribution is specific. The extreme values of the stress are arranged pointwise at the contractions in the scarf joint. In the case of the dry pine wood, these stress is almost unnoticeable in relation to the stress distribution observed in the wet wood (figures 6-7). The analysed joint have antisymmetric maximal principal stress distribution (Types 2 and 3) in wet wood and the maximum principal values of stresses are approximately 84 MPa (figure 6b-7b). The maximal principal stress in the saddle notch corner joint made of both dry and wet pine wood is distributed symmetrically for all types of boundary conditions (figure 10-11).

In addition to the described stress distributions, the distinct displacements between logs have been observed in the short-corner dovetail connection with Type 2 and 3 of the boundary conditions (figure 7).

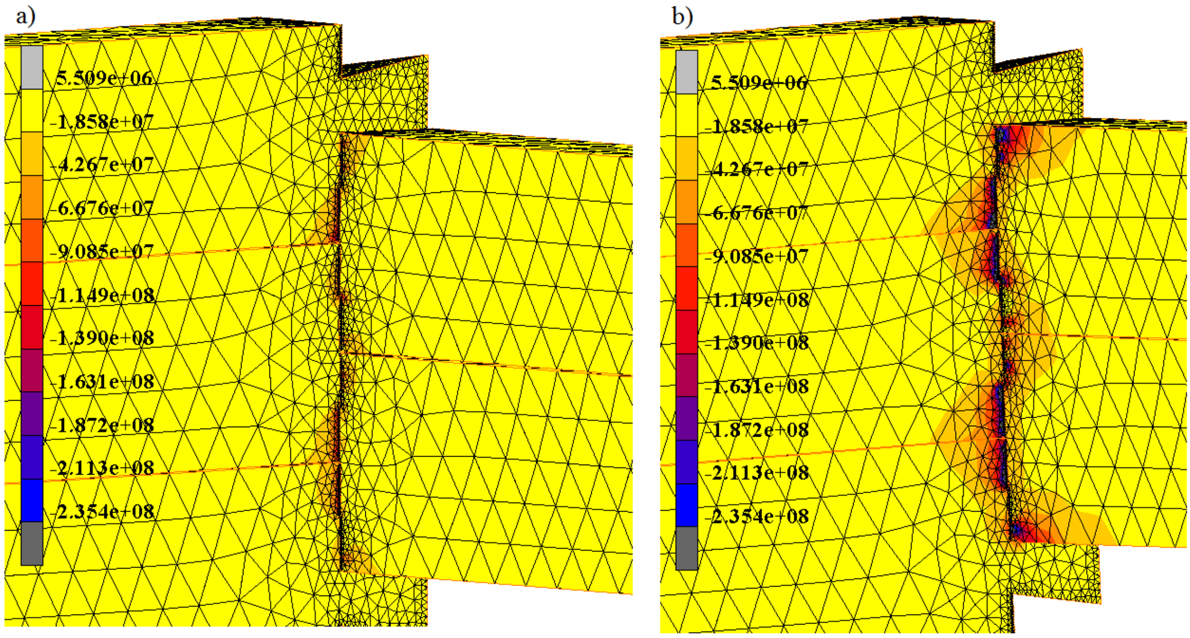

Figure 4: Minimum principal stress [Pa] distribution in the corner of short-corner dovetail connection for Type 1 of boundary conditions for: a) dry wood, b) wet wood

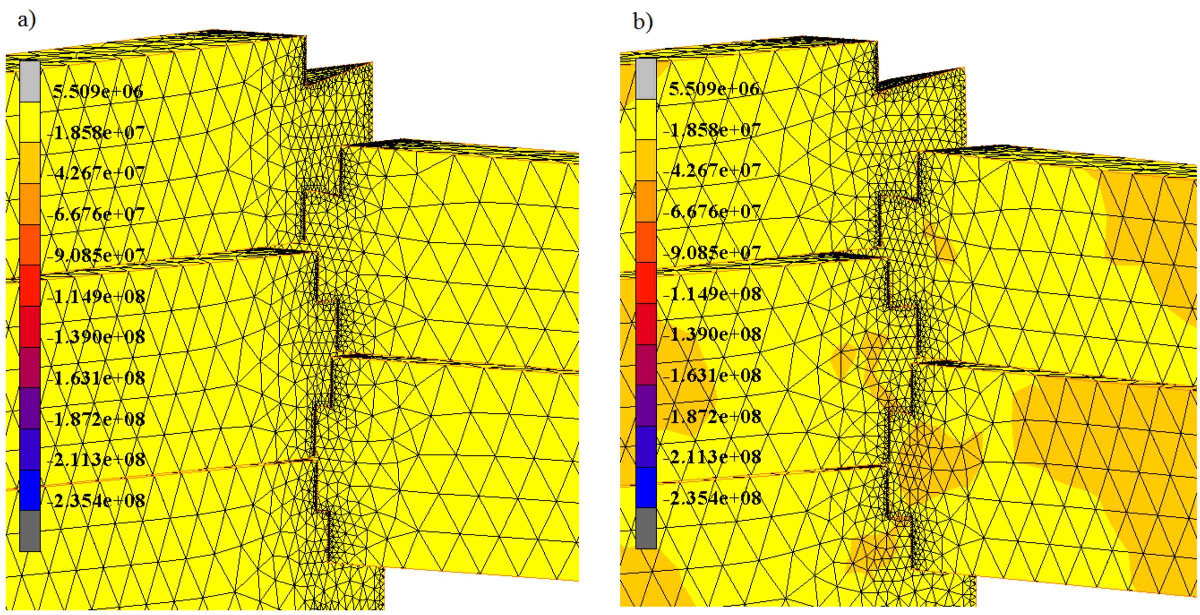

Figure 5: Minimum principal stress [Pa] distribution in the corner of short-corner dovetail connection for Type 2 of boundary conditions for: a) dry wood, b) wet wood

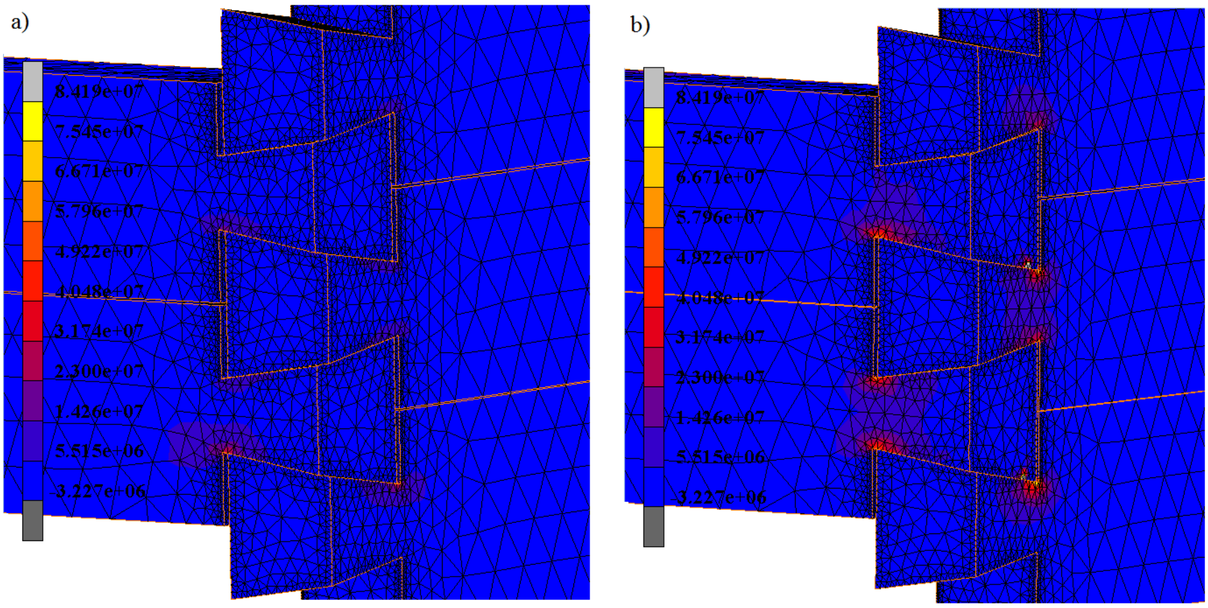

Figure 6: Maximum principal stress [Pa] distribution in the corner of short-corner dovetail connection for Type 1 of boundary conditions for: a) dry wood, b) wet wood

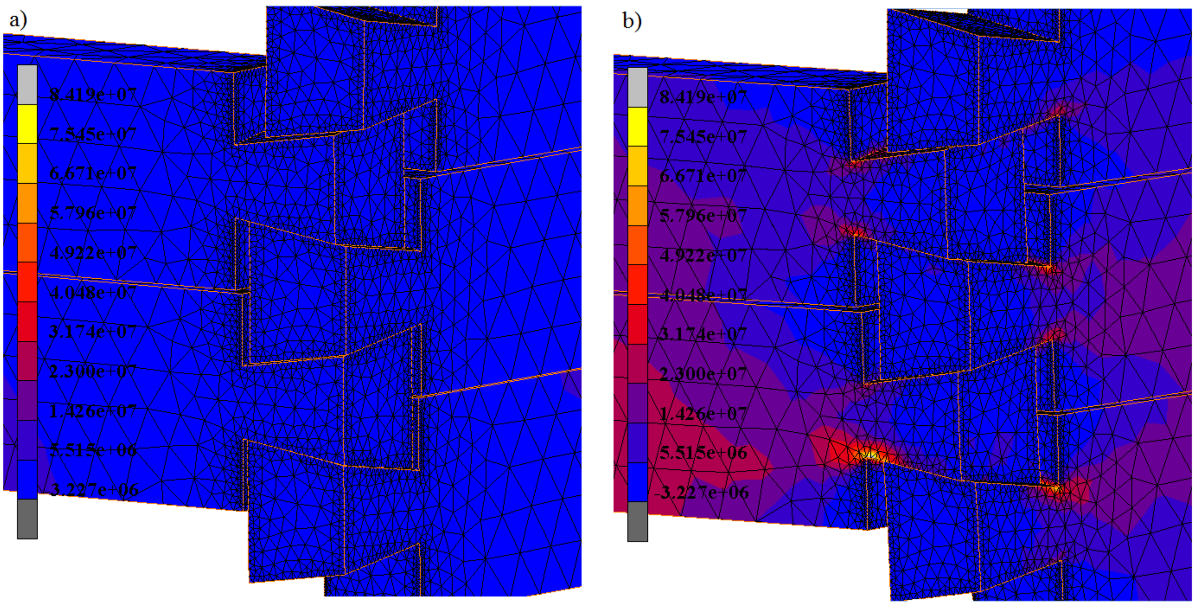

Figure 7: Maximum principal stress [Pa] distribution in the corner of short-corner dovetail connection for Type 2 of boundary conditions for: a) dry wood, b) wet wood

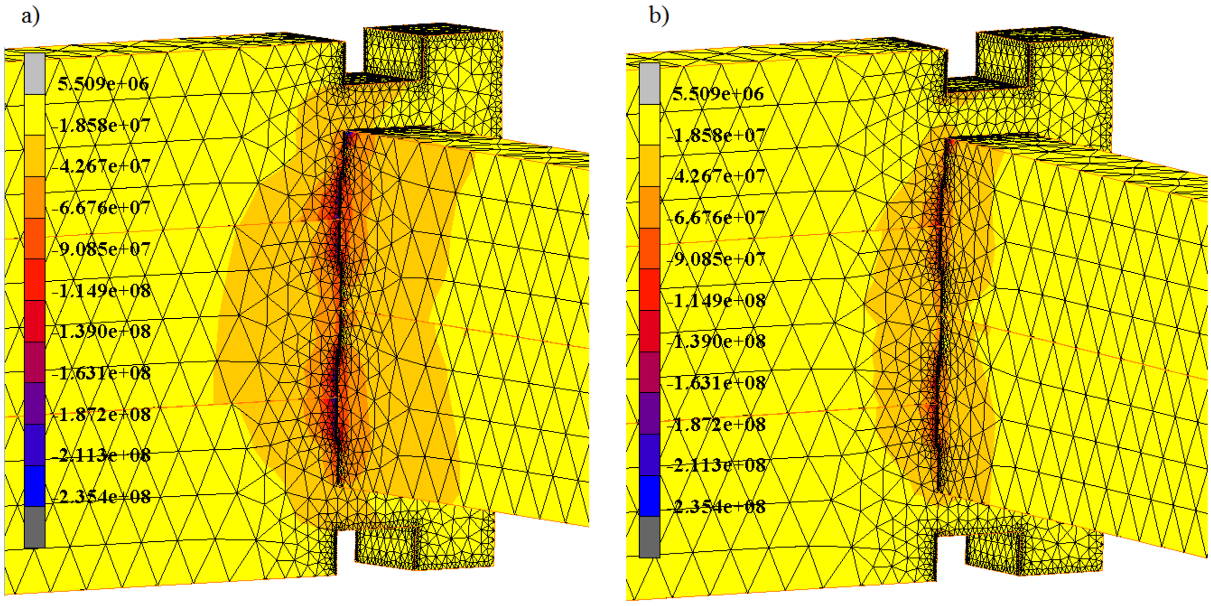

Figure 8: Minimum principal stress [Pa] distribution in the corner of saddle notch corner joint for Type 1 of boundary conditions for: a) dry wood, b) wet wood

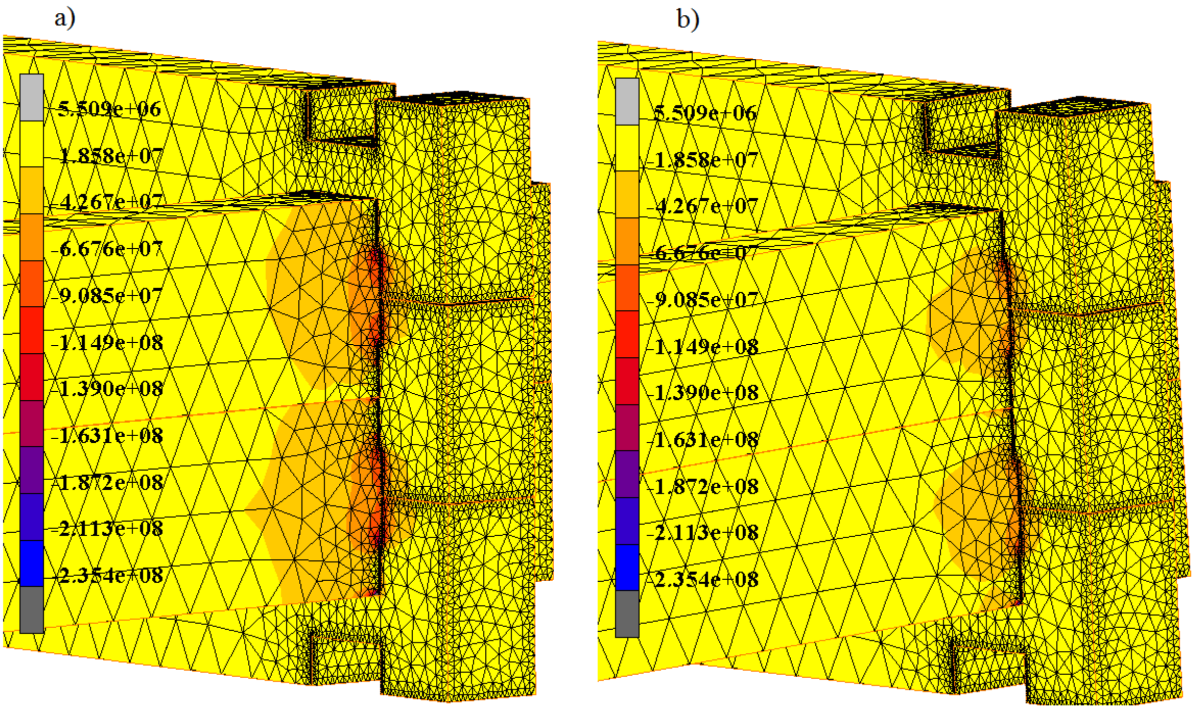

Figure 9: Minimum principal stress [Pa] distribution in the corner of saddle notch corner joint for Type 2 of boundary conditions for: a) dry wood, b) wet wood

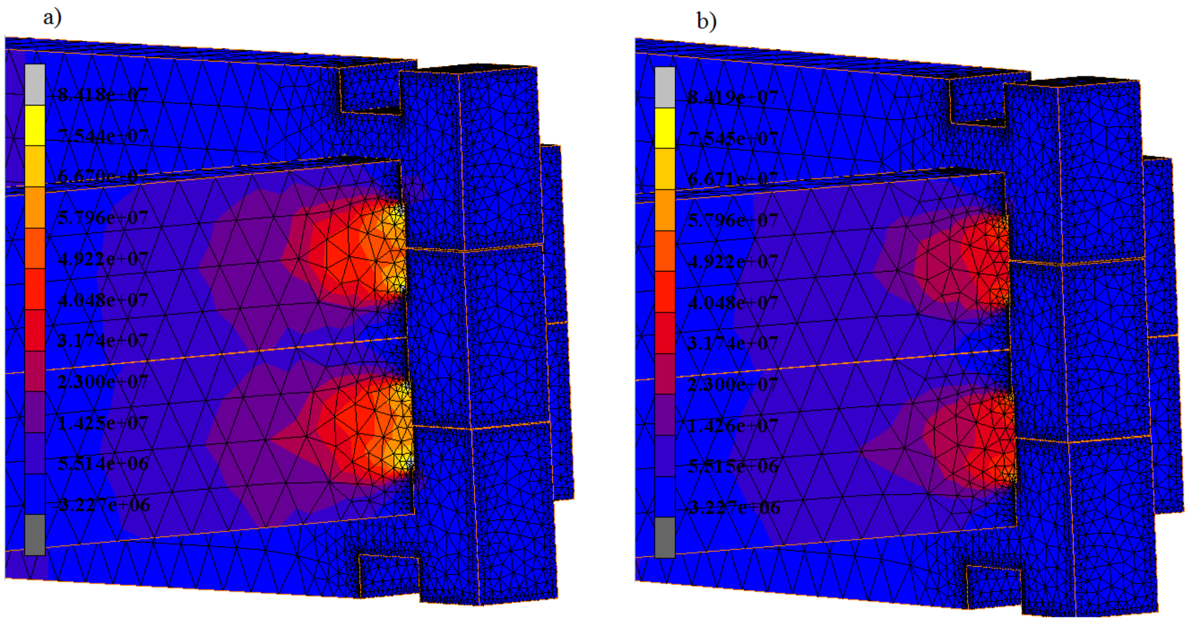

Figure 10: Maximum principal stress [Pa] distribution in the corner of saddle notch corner joint for Type 1 of boundary conditions for: a) dry wood, b) wet wood

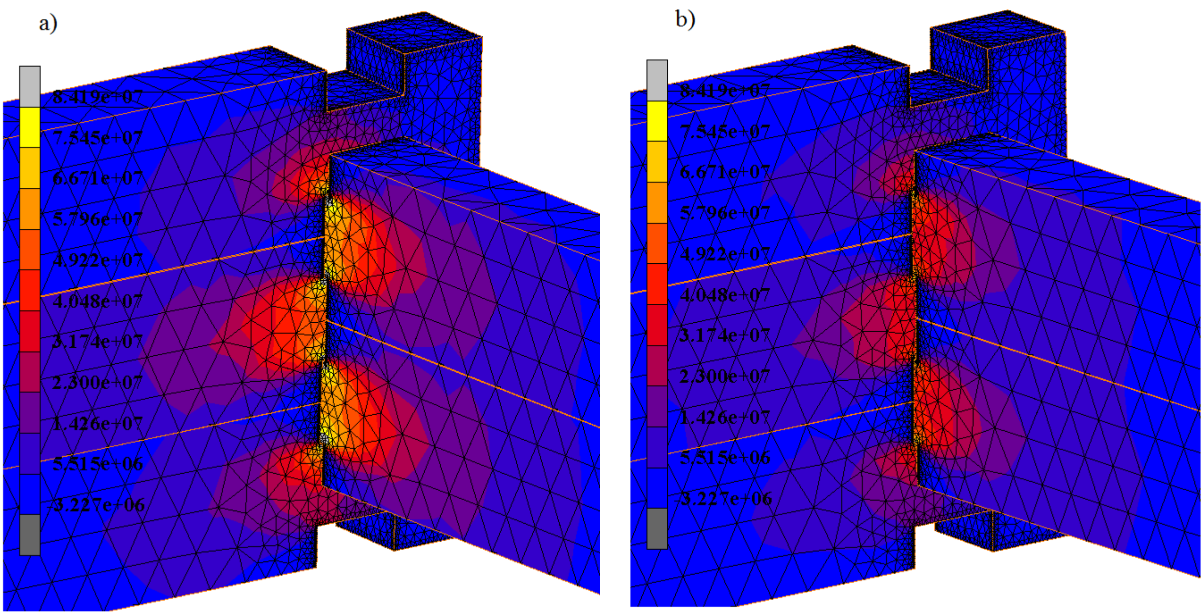

Figure 11: Maximum principal stress [Pa] distribution in the corner of saddle notch corner joint for Type 2 of boundary conditions for: a) dry wood, b) wet wood

4 CONCLUSIONS

One of the most popular carpentry joint preserved in structures of wooden architecture have been analysed with four types of boundary conditions and as a dry and wet pine wood variants. On the basis of the numerical analysis, the highest stress areas have been established. In the corner of the analysed connection, the minimum principal stress distributions have been observed from the inside of the joint. In turn, the maximum principal stress distributions can be observed from the outside of the connection. It has been noticed that the results are identical for the joints loaded in two different ways. The first, where the same values of the forced displacements is applied along the logs (Types 1 and 2) and the second, where it is applied perpendicularly to them (Type 4 and 3). Type 1 corresponds to Type 4 and Type 2 corresponds to 3. In the case of the short-corner dovetail joint made of wet pine wood, the stress concentration area in the connection corner is larger than in this joint made of dry pine wood. Also the maximum values of stress are higher in the wet than in the dry wood. The opposite phenomenon has been observed in saddle notch joint. It has been noted that both minimum and maximum principal values of stress are the highest when Type 1 and 4 of boundary conditions are applied to the joints independently of the wood moisture. The obtained compressive stress values are much higher than the tensile stress values. For analysed types of boundary conditions in both considered joints, the vulnerable damage zones are probably in the same places where the high stress areas are observed in the numerical results.

On the basis of the obtained stress values, Types 1 and 4 of boundary conditions are more unfavourable due to the possible destruction along the edges of the logs. In turn, the deformations in the connection corner are greater for Type 2 and 3 of the boundary conditions in relation to Type 1 and 4. These type of displacements of the logs exposes the inside surfaces of the logs to environmental and biological degradation, so it may be particularly dangerous for the joint and the structure.

ACKNOWLEDGMENT

This work has been partially supported by the National Science Centre, Poland (grant No. 2015/17/B/ST8/03260) and by the subsidy for development of young scientists given by the Faculty of Civil and Environmental Engineering, Gdańsk University of Technology.

REFERENCES

[1] Green, D.W., Winandy, J.E., Kretschmann, D.E. *Wood handbook – Wood as an Engineering Material*. Madison (1999).

[2] Nowak, T.P., Jasieńko, J., Hamrol-Bielecka, K. In situ assessment of structural timber using the resistance drilling method - Evaluation of usefulness. *Constr. Build. Mater.* (2016) **102**:403–415.

[3] Michniewicz, W. *Konstrukcje drewniane (Wooden construction).* Arkady, Warsaw (1958).

[4] Lacki, P., Derlatka A. Analiza numeryczna konstrukcji drewnianej jako struktury ortotropowej (Numerical analysis of timber structure as an orthotropic material). in: *Scientific Papers of Czestochowa University of Technology* (2013) 69–76.

[5] Sonderegger, W., Kránitz, K., Bues, C., Niemz, P. Aging effects on physical and

mechanical properties of spruce, fir and oak wood. *J. Cult. Herit.* (2015) **16**:883–889.
[6] Morales-Conde, M.J., Machado, J.S., Evaluation of cross-sectional variation of timber bending modulus of elasticity by stress waves. *Constr. Build. Mater.* (2017) **134**:617–625.
[7] Phleps, H. *Holzbaukunst der Blockbau.* Karlsruhe (1942).
[8] Cielatkowska, R. *Translocatio. Przeniesienie drewnianych świątyń trzech obrządków. (Translocatio Transfer of wooden temples of the three religions).* Department of Architecture of Gdansk University of Technology, (Gdansk 2014).
[9] Jasieńko, J., Nowak, T., Karolak, A. Historyczne z łą cza ciesielskie (Historical carpentry joints). *J. Herit. Conserv.* (2014) **40**:58–82.
[10] Repelewicz, A. Traditional carpenter's roofs. *Sci. Pap. Czestochowa Univ. Technol.* (2013) **19**:150–155.
[11] Aira, J.R., Arriaga, F., Íñiguez-González, G., Guaita, M. Failure modes in halved and tabled tenoned timber scarf joint by tension test. *Constr. Build. Mater.* (2015) **96**:360–367.
[12] Sangree, R.H., Schafer, B.W. Experimental and numerical analysis of a halved and tabled traditional timber scarf joint. *Constr. Build. Mater.* (2009) **23**:615–624.
[13] Palma, P., Garcia, H., Ferreira, J., Appleton, J., Cruz, H. Behaviour and repair of carpentry connections – Rotational behaviour of the rafter and tie beam connection in timber roof structures. *J. Cult. Herit.* (2012) **13**:S64–S73.
[14] Palma, P., Ferreira, J., Cruz, H. Monotonic tests of structural carpentry joints, in: *World Conference on Timber Engineering (WCTE)* (2010) 1–6.
[15] Calderoni, C., De Matteis, G., Giubileo, C., Mazzolani, F.M. Experimental correlations between destructive and non-destructive tests on ancient timber elements. *Eng. Struct.* (2010) **32**:442–448.
[16] Calderoni, C., De Matteis, G., Giubileo, C., Mazzolani, F.M. Flexural and shear behaviour of ancient wooden beams: Experimental and theoretical evaluation. *Eng. Struct.* (2006) **28**:729–744.
[17] Jasieńko, J., Engel, L., Rapp, P. Study of stresses in historical carpentry joints by photoelasticity modelling, in: Lourenço (Ed.), *Structural Analysis of Historical Constructions, Possibilities of Numerical and Experimental Techniques,* Macmillan India Ltd., New Delhi, 6-8 November (2006).
[18] Jasieńko, J., Engel, L., Gospodarek, T. Elastooptische und numerische Undersuchungen ausgewählter Verbindungen an hölzerner Denkmalkonstruktionen, in: *VI. Deutsch-Polnische Konferenz ANTIKON 2005 Wismar*, Wiesmar (2005).
[19] Jasieńko, J., Kardysz, M. Deformation and strength criteria in assessing mechanical behaviour of joints in historic timber structures. in: *Proceedings of the 16th International Conference: From Material to Structure – Mechanical Behaviour and Failures of the Timber Structures, ICOMOS International Wood Committee* (2007) 218–230.
[20] Humbert, J., Boudaud, C., Baroth, J., Hameury, S., Daudeville, L. Joints and wood shear walls modelling I: Constitutive law, experimental tests and FE model under quasi-static loading. *Eng. Struct.* (2014) **65**:52–61.
[21] Boudaud, C., Humbert, J., Baroth, J., Hameury, S., Daudeville, L. Joints and wood shear walls modelling II: Experimental tests and FE models under seismic loading.

Eng. Struct. (2015) **101**:743–749.

[22] Armesto, J., Lubowiecka, I., Ordóñez, C., Rial, F.I. FEM modeling of structures based on close range digital photogrammetry. *Autom. Constr.* (2009) **18**: 559-569.

[23] Rajczyk, M., Jończyk, D., Analiza numeryczna belki drewnianej (Numerical analysis of timber beam). *Sci. Pap. Czestochowa Univ. Technol.* (2014) **20**:231–239.

[24] Trochonowicz, M., Kołodziejczuk, N. Wpływ temperatury, wilgotności i kierunku badań na war tość współczynnika przewodności cieplnej λ w róż nych gatunkach drewna (The impact of temperature, humidity and the direction of analysis on thermal conductivity λ in different types of wood). *Bud. I Archit.* (2015) **14**:149–156.

[25] Kozakiewicz, P., *Effects of temperature and humidity on the compressive strength along fibres selected types of wood of varying density and anatomical structure*, SGGW Publisher, Warsaw (2010).

[26] Villar, J.R., Guaita, M., Vidal, P., Arriaga, F. Analysis of the Stress State at the Cogging Joint in Timber Structures. *Biosyst. Eng.* (2007) **96**: 79–90.

[27] Schmidt, J., Kaliske, M., Models for numerical failure analysis of wooden structures. *Eng. Struct.* (2009) **31**:571–579.

[28] Klein, A., Grabner, M. Analysis of Construction Timber in Rural Austria: Wooden Log Walls. *Int. J. Archit. Herit.* (2015) **9**:553–563.

[29] Nowak, T.P., Jasieńko, J., Czepizak, D. Experimental tests and numerical analysis of historic bent timber elements reinforced with CFRP strips. *Constr. Build. Mater.* (2013) **40**:197–206.

[30] Kopkowicz, F. *Ciesielstwo polskie (Polish carpentry).* Arkady, Warsaw (1958).